

**REPORT DOCUMENTATION PAGE**
*Form Approved  
OMB No. 0704-0188*

The public reporting burden for this collection of information is estimated to average 1 hour per response, including the time for reviewing instructions, searching existing data sources, gathering and maintaining the data needed, and completing and reviewing the collection of information. Send comments regarding this burden estimate or any other aspect of this collection of information, including suggestions for reducing the burden, to Department of Defense, Washington Headquarters Services, Directorate for Information Operations and Reports (0704-0188), 1215 Jefferson Davis Highway, Suite 1204, Arlington, VA 22202-4302. Respondents should be aware that notwithstanding any other provision of law, no person shall be subject to any penalty for failing to comply with a collection of information if it does not display a currently valid OMB control number.

**PLEASE DO NOT RETURN YOUR FORM TO THE ABOVE ADDRESS.**

1. REPORT DATE (DD-MM-YYYY) 04/26/2011	2. REPORT TYPE Quarterly Progress Report	3. DATES COVERED (From - To) 1/26/2010-4/25/2011		
4. TITLE AND SUBTITLE Simultaneous Extraction of Lithium and Hydrogen from Seawater		5a. CONTRACT NUMBER N00014-10-M-0234 5b. GRANT NUMBER 5c. PROGRAM ELEMENT NUMBER 5d. PROJECT NUMBER 20126083 5e. TASK NUMBER 0001AC 5f. WORK UNIT NUMBER		
6. AUTHOR(S) Dr. Pyoungho Choi		8. PERFORMING ORGANIZATION REPORT NUMBER Quarterly Progress Report for Period January 26, 2010-April 25, 2011		
7. PERFORMING ORGANIZATION NAME(S) AND ADDRESS(ES) University of Central Florida/Florida Solar Energy Center 1679 Clearlake Road Cocoa FL 32922-5703		10. SPONSOR/MONITOR'S ACRONYM(S) ONR		
9. SPONSORING/MONITORING AGENCY NAME(S) AND ADDRESS(ES) Office of Naval Research ONR 253 875 N. Randolph Street Arlington, VA 22203-1995		11. SPONSOR/MONITOR'S REPORT NUMBER(S) 0001AC		
12. DISTRIBUTION/AVAILABILITY STATEMENT Distribution Statement A: Approved for public release. Distribution is unlimited. Report dated 4/26/2011.				
13. SUPPLEMENTARY NOTES				
14. ABSTRACT The goal is to demonstrate a novel electrolytic process for extracting Li from seawater. The technical objectives are to prove the concept of electrolytic process and to develop effective membranes for the diffusion of lithium ion from natural seawater to an extractant. Process variables are potential applied between seawater and fresh water, flow rates, and the ratio of the volume of anolyte to that of cathoyte in the flow system.				
15. SUBJECT TERMS				
16. SECURITY CLASSIFICATION OF: a. REPORT		17. LIMITATION OF ABSTRACT	18. NUMBER OF PAGES 12	19a. NAME OF RESPONSIBLE PERSON Dr. Pyoungho Choi 19b. TELEPHONE NUMBER (Include area code) 321-638-1436

## Quarterly Progress Report 3

### Project Title: Simultaneous Extraction of Lithium and Hydrogen from Seawater

**Project Period:** 7/26/2010 – 7/25/2011

**Reporting Period:** January 26, 2010 – April 25, 2011

**Date of Report:** April 26, 2011

**Recipient:** University of Central Florida

**Award Number:** N00014-10-M-0234

**Contact:** Pyoungho Choi, UCF, 321 638-1436, [pchoi@fsec.ucf.edu](mailto:pchoi@fsec.ucf.edu)

**Program Officer:** Dr. Michele Anderson, ONR Code: 332, [michele.anderson1@navy.mil](mailto:michele.anderson1@navy.mil)

#### Project Goal:

Seawater is a source of lithium and also is ultimate source of clean and renewable hydrogen. The goal is to develop a seawater electrolysis process with its potential for simultaneously extracting lithium during the electrolysis.

#### Hydrogen Generation by Seawater Electrolysis:

Seawater contains salts of less than 35 salinity (g salt/kg solution) and seawater electrolysis (SWE) technology lies between the two well-known technologies, namely, water (or fresh water) electrolysis and the brine electrolysis using a solution containing 350 salinity (g salt/kg solution) [1-10]. While the SWE can be carried out either desalination of sea water and followed by the well-established fresh water electrolysis or direct electrolysis of sea water, the latter seems more attractive because the desalination often employs the reverse osmosis process that not only requires additional cost but also causes environmental problems.

Seawater electrolysis is different from that of fresh water splitting, due to ions present in seawater, e.g.,  $\text{Na}^+$ ,  $\text{Ca}^{2+}$ , and  $\text{Mg}^{2+}$ .

Figure 1 shows a configuration of the seawater electrolysis. Seawater and fresh water are introduced to the anode and cathode side, respectively. Hydrogen and oxygen are produced at the cathode and anode surface, respectively. At the anode, oxygen as well as chlorine gas can be produced, while the hydrogen is generated at the cathode. The oxygen evolution at the anode is thermodynamically favorable to the chlorine generation

Anode reaction:



Cathode reaction:



However, the kinetics of the chlorine generation is much faster than that of oxygen evolution, i.e., the ratio of exchange current densities of chlorine to oxygen production is in the range of  $10^3$ - $10^7$ . Thus, at high potentials, e.g.,  $> 2.0$  V, the chlorine gas may be evolved exclusively [11-20]. However, the two reactions competitive as the concentration of reacting water molecule is much higher than that of chlorine ions near the electrode surface.

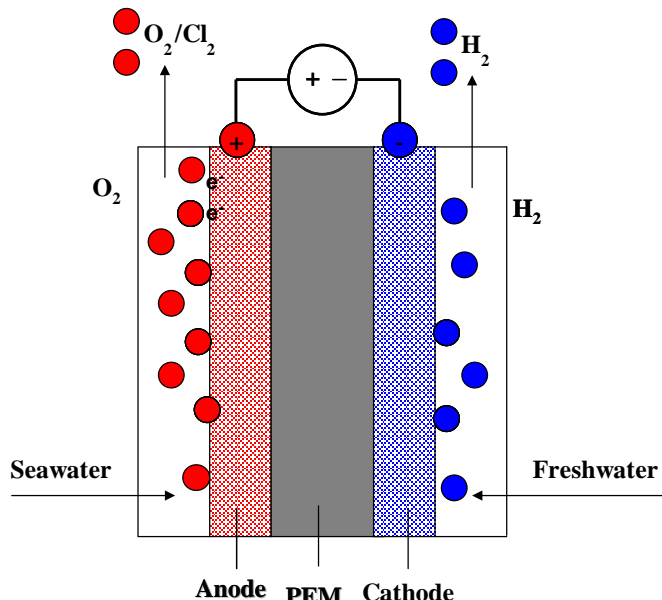


Figure 1. Schematic of electrolytic cell extracting  $\text{Li}^+$  ion from seawater.

During the SWE,  $\text{Ca}^{2+}$  and  $\text{Mg}^{2+}$  ions may be participate in the following reactions,



which may result in solid deposits of  $\text{Ca}(\text{OH})_2$  and  $\text{Mg}(\text{OH})_2$  on the cathode surface. The formation of the deposits may inhibit the diffusion of reacting species to the electrode surface and blocks the active site of cathode for the hydrogen generation reaction.

In this study, we have examined Pt, Ir, and Ni electrodes on the performance of the seawater electrolysis. The hydrogen generation rate at the cathode, current efficiency, and polarization characteristics have been studied. Further, we have incorporated a lithium-ion conducting material into the anode to investigate the lithium diffusion and extraction.

### **Experimental:**

Synthesis of  $\text{Li}^+$  adsorbents: lithium adsorbing ion-sieve  $\text{LiMg}_{0.5}\text{Mn}_{1.5}\text{O}_4$  was prepared by solid state reaction. 6.1g of  $\text{Li}_2\text{CO}_3$ , 8.9g of  $\text{Mg}(\text{CH}_3\text{COO})_2 \cdot 4\text{H}_2\text{O}$  and 5.6g of  $\text{MnCO}_3$  were mixed, ball milled for 2 hours, and calcined at  $600^\circ\text{C}$  for 4 hours.

Synthesis of Lisicon: the lithium ion-conducting materials were prepared from the mixture of  $\text{Li}_2\text{S}$  and  $\text{P}_2\text{S}_5$  crystalline powders. The mixture was mechanically mixed using a ball mill

apparatus (Retsch PM100). The powders were heated to 230°C and kept at the temperature for 4 hours, and slowly cooled down.

MEA preparation: Iridium (Ir) was used as the anode and Pt/C (Tanaka, 45.5wt.% Pt), or Ir, or Raney-Ni was used as the cathode. The Lisicon (or adsorbents) were mixed with Ir by 20wt.% for lithium extraction process. MEAs were prepared by spraying the electrode onto diffusion layers using a spraying technique. The catalyst ink was prepared with 180mg catalyst, 5g methanol, water, and 1.54g of 5wt.% solubilized Nafion® solution (EW1100, supplied by Ion Power): this gives 30% ionomer in the catalysts layer. The loadings were 3.0mg/cm<sup>2</sup> and 1.5mg/cm<sup>2</sup>, for the anode and cathode, respectively. The NRE 212 membrane was “sandwiched” between electrode-coated diffusion layers.

Electrochemical measurement: The electrochemical measurements of the seawater electrolysis were carried out in a PEM electrolyzer under galvanostatic conditions. Seawater and deionized water was used as the anolyte and catholyte, respectively. Cell currents were set at 10 mA/cm<sup>2</sup>, or 20 mA/cm<sup>2</sup>, or 50 mA/cm<sup>2</sup>, or 100 mA/cm<sup>2</sup> and resulting voltages were recorded with time. Anolyte as well as catholyte from the cell was collected every five minutes for the analysis of ions present in the effluents.

Measurement of hydrogen gas produced: Hydrogen and oxygen gases coming out of the cell were collected and the amount was measured volumetrically.

Ion chromatography: Ions in seawater diffused from/to the anode and cathode were determined by ion chromatography. Anions were analyzed by Anion Ion Chromatography (Instrument Dionex ICS-1500, Column Dionex AS9-HC; AG9-HC Guard, eluent: 9.00 mM Na<sub>2</sub>CO<sub>3</sub>, flow rate: 1.25 mL/min, and sample loop was 25 µL). Cations were analyzed by Cation Ion Chromatography (Instrument Dionex DX-500, Cation Column Dionex CS12A; CG12A Guard, eluent: 20.00 mM methanesulfonic acid, flow rate: 1.25 mL/min, and sample loop: 25 µL).

Electrolytic Cell: An electrolytic cell was made by incorporating the cell components with a two-pump flow system.

## Results & Discussion

Iridium is used as the anode as it selectively generates oxygen over chlorine in seawater electrolysis. Figure 2 shows the electrochemical activity of various MEAs consisted of Pt, or Ir or Raney-Ni cathodes at 10mA/cm<sup>2</sup>. At the low current density, the cell potential was in the range of 2.1-2.3V and it was stable over time. Raney-Ni is inexpensive and is as active as precious metals for seawater electrolysis. Figure 3 shows the amount of hydrogen generated at the constant current density. The volume of the hydrogen gas increases with time. The solid line represents the theoretical amount of gases calculated from the applied current density based on the assumption that the electrons produced in the reaction 1 contribute to the formation of hydrogen by the reaction 3 or 4.

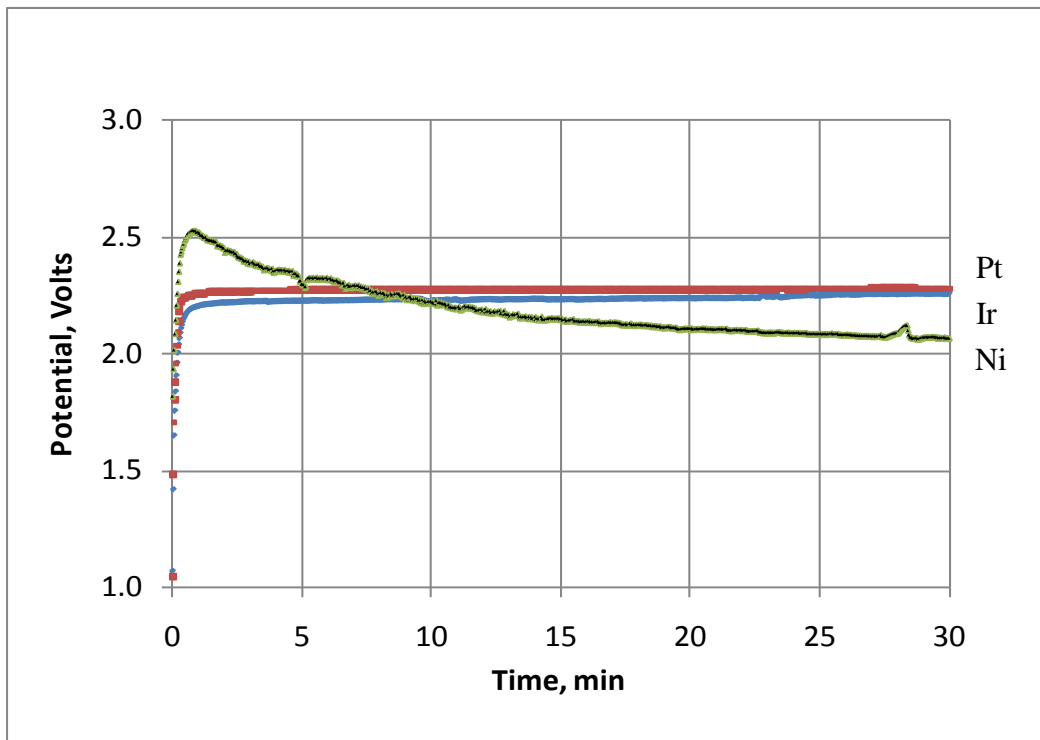


Figure 2. Potential responses to constant current density of  $10\text{mA/cm}^2$  (anode:  $3.0\text{mg Ir/cm}^2$ , cathode: Pt, Ir, Ni  $1.5\text{mg /cm}^2$ , anolyte: seawater, catholyte: fresh water, and cell temp.:  $20^\circ\text{C}$ ).

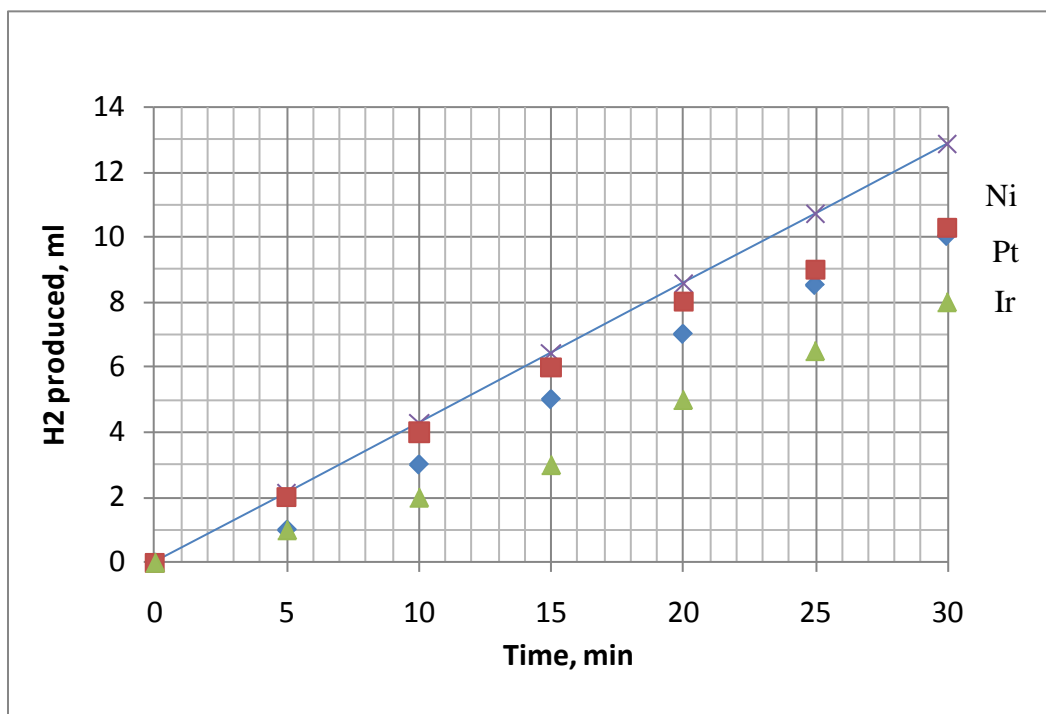


Figure 3. Volume of hydrogen gas produced at  $10\text{ mA/cm}^2$  (anode:  $3.0\text{mg Ir/cm}^2$ , cathode: Pt, Ir, Ni  $1.5\text{mg /cm}^2$ , anolyte: seawater, catholyte: fresh water, and cell temp.:  $20^\circ\text{C}$ ).

Figure 4 shows the potential changes under a constant current density of  $100\text{mA/cm}^2$ . Clearly, Ir cathode shows the lowest potential among the electrodes. The electrodes are stable and no increase in resistance or potential was observed during the electrolysis. As Raney-Ni is a low cost material, it may be utilized in practice.

Table 1 shows the averaged current efficiency for hydrogen generation at three different current densities. At low current density, Ni and Pt show higher efficiency than Ir does. However, the efficiency is more than 90% at  $100\text{mA/cm}^2$  for all the cathodes.

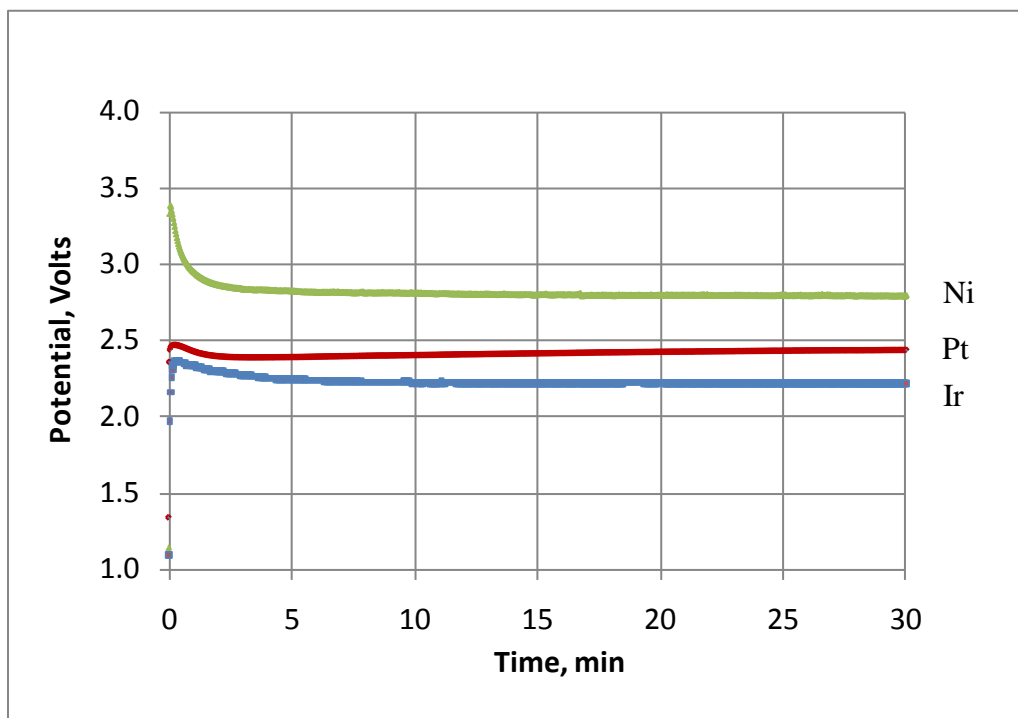


Figure 4. Potential responses at constant current density of  $100\text{mA/cm}^2$  (anode:  $3.0\text{mg Ir/cm}^2$ , cathode: Pt, Ir, Ni  $1.5\text{mg /cm}^2$ , anolyte: seawater, catholyte: fresh water, and cell temp.:  $20^\circ\text{C}$ ).

Table 1. Current efficiency for hydrogen generation

	Averaged Current Efficiency, %		
	$10\text{mA/cm}^2$	$50\text{mA/cm}^2$	$100\text{mA/cm}^2$
Pt	71.0	91.4	92.7
Ir	51.8	86.7	92.2
Ni	89.5	77.4	90.4

### **Ion Chromatogram Analysis of Catholyte**

Figure 5 shows IC chromatogram of catholyte after 30 minutes of operation;  $\text{Na}^+$ ,  $\text{K}^+$ ,  $\text{Mg}^{2+}$  and  $\text{Ca}^{2+}$  ions were clearly separated. Due to relatively high  $\text{Na}^+$  concentration in seawater and non-selective diffusion of ions from the anolyte (seawater) to the catholyte (freshwater), the  $\text{Li}^+$  peak was not separately detected.

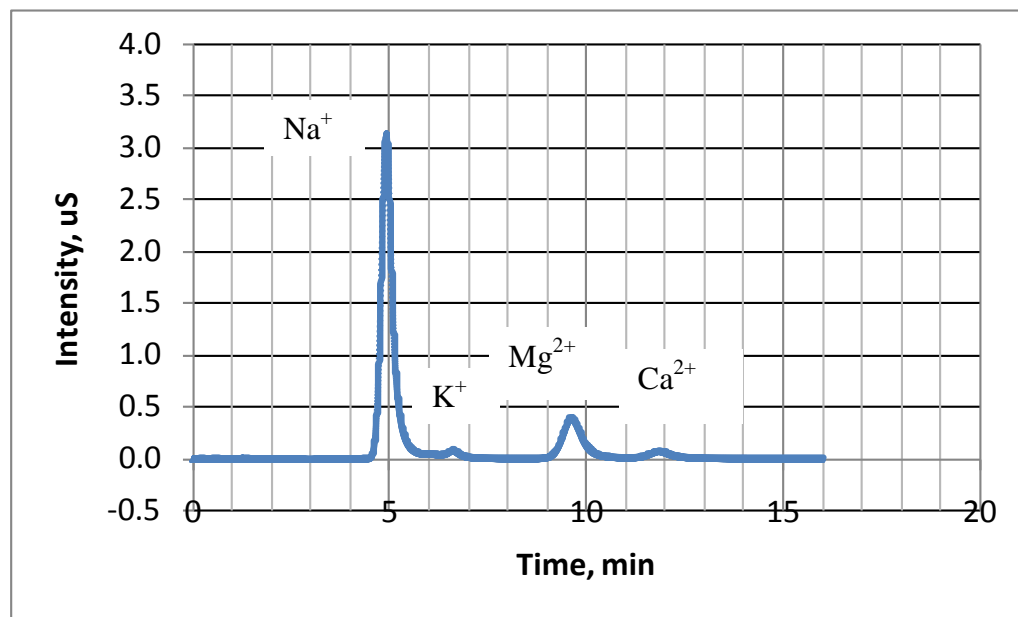


Figure 5. IC chromatogram of catholyte (Anode: Ir, 3mg/ccm<sup>2</sup>, cathode: Pt, 1.5mg/cm<sup>2</sup>, anolyte: seawater, catholyte: fresh water).

Figure 6 and 7 show the areas of  $\text{Na}^+$  ion in the cathode side as a function of time for Pt, Ir and Ni cathode when Ir was used as the anode. At 100mA/cm<sup>2</sup>, high concentration of  $\text{Li}^+$  ions was observed in the cathode effluent. For example, the area of  $\text{Na}^+$  ions for Pt cathode after thirty minutes of electrolysis was 1.05 uS\*min when the cell was operated at 100mA/cm<sup>2</sup>, while it was 0.14 uS\*min at 10mA/cm<sup>2</sup> condition. This is attributed to the higher potential across the cell at high current density operation. Pt cathode shows high rate of diffusion at 100mA/cm<sup>2</sup>. The concentration of  $\text{Na}^+$  in the catholyte at low current density of 10mA/cm<sup>2</sup> was almost the same when Pt, or Ir, or Ni was employed as the cathode.

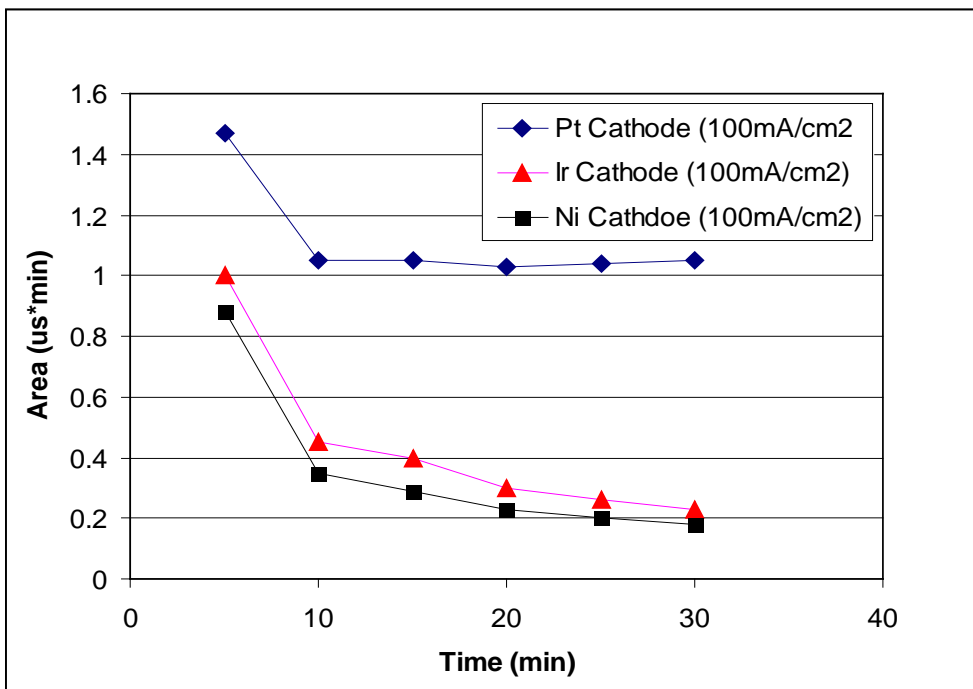


Figure 6. Area of the  $\text{Na}^+$  ion in the cathode effluent with time at  $100\text{mA}/\text{cm}^2$  (anode:  $3.0\text{mg Ir}/\text{cm}^2$ , cathode: Pt, Ir, Ni  $1.5\text{ mg}/\text{cm}^2$ ,  $T=20^\circ\text{C}$ ).

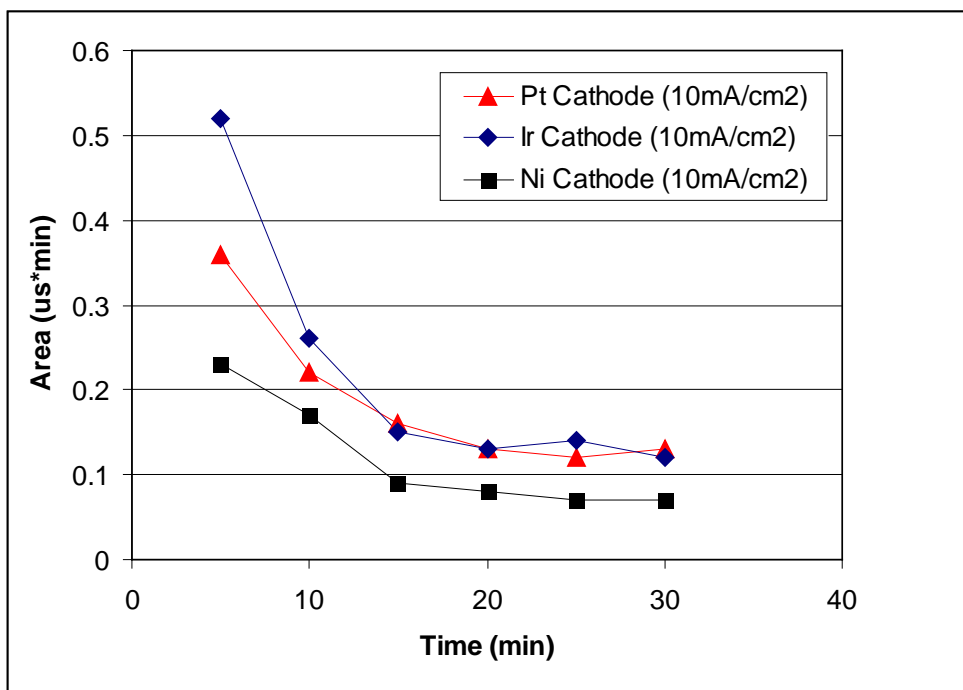


Figure 7. Area of the  $\text{Na}^+$  ion in the cathode effluent with time at  $10\text{mA}/\text{cm}^2$  (anode:  $3.0\text{mg Ir}/\text{cm}^2$ , cathode: Pt, Ir, Ni  $1.5\text{ mg}/\text{cm}^2$ ,  $T=20^\circ\text{C}$ ).

Table 2 shows the percentage of ions diffused from the anolyte to the catholyte. The amount of ions diffused was less than 0.1% for all the conditions. The rate of ionic diffusion depends on the current applied and electrode materials used.

Table 2. Percentage of  $\text{Na}^+$  diffused to catholyte at  $10\text{mA}/\text{cm}^2$  and  $100\text{mA}/\text{cm}^2$

Time	Percentage of $\text{Na}^+$ ion diffused to the catholyte @ $100\text{ mA}/\text{cm}^2$ , %			Percentage of $\text{Na}^+$ ion diffused to the catholyte @ $10\text{ mA}/\text{cm}^2$ , %		
	Pt	Ir	Ni	Pt	Ir	Ni
5	0.088	0.060	0.053	0.021	0.031	0.014
10	0.063	0.027	0.021	0.013	0.016	0.010
15	0.062	0.024	0.017	0.010	0.009	0.005
20	0.062	0.018	0.014	0.008	0.008	0.005
25	0.062	0.016	0.012	0.007	0.008	0.004
30	0.063	0.014	0.011	0.008	0.007	0.004

### Effect of Lisicon incorporated into Anode Materials on $\text{Li}^+$ Diffusion

Figure 8 shows the potential changes at  $100\text{mA}/\text{cm}^2$  when Lisicon was mixed with Ir anode. The activity of the anode is slightly lower than that of Ir only. The electrode is stable and about 2.5V potential is required to maintain the current density. The ion chromatogram of the cathode effluent was shown in Figure 9. Lithium ion ( $\text{Li}^+$ ) was separately detected and its area was shown in Table 3.

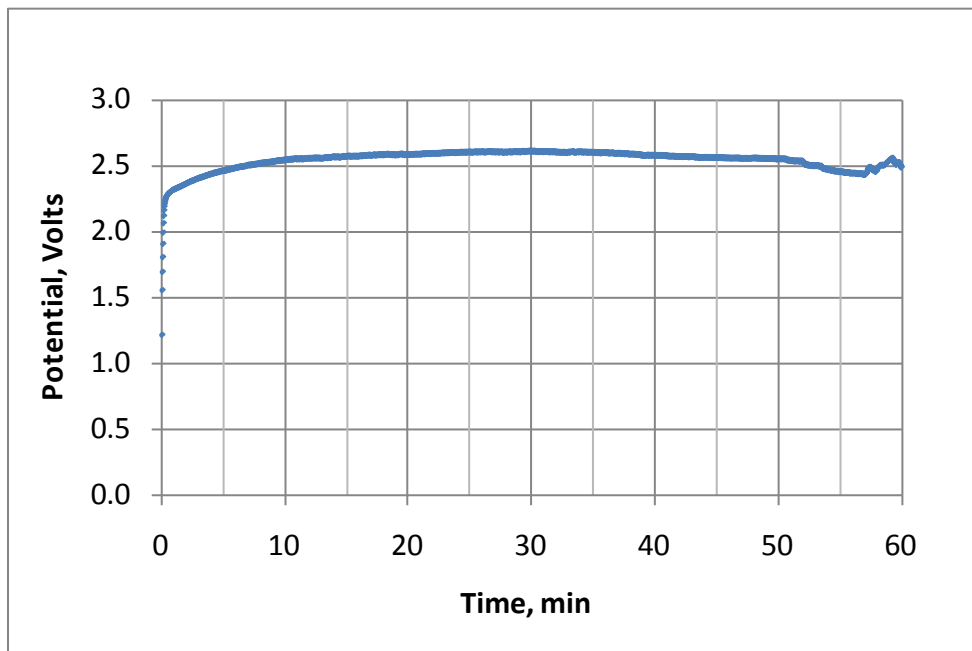


Figure 8. Potential responses at constant current density of  $100\text{mA}/\text{cm}^2$  (anode: 20 wt. % Lisicon and 80 wt.% Ir,  $3.0\text{mg}/\text{cm}^2$ , cathode: Ir  $1.5\text{mg}/\text{cm}^2$ , anolyte: seawater, catholyte: fresh water, and cell temp.:  $20^\circ\text{C}$ ).

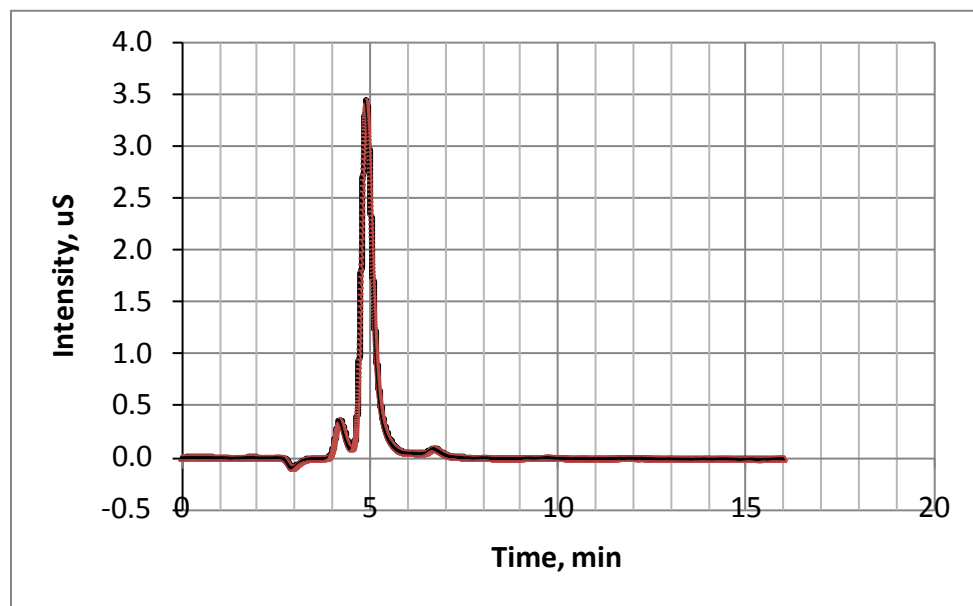


Figure 9. IC chromatogram of catholyte (Anode: Ir, 3mg/ccm<sup>2</sup>, cathode: Pt, 1.5mg/cm<sup>2</sup>, anolyte: seawater, catholyte: fresh water).

Compared to Ir anode, the incorporation of the Li<sup>+</sup> ion-conducting material increases the rate of diffusion of Li<sup>+</sup> ions.

Table 3. Percentage of Na<sup>+</sup> diffused to catholyte at 10mA/cm<sup>2</sup> and 100mA/cm<sup>2</sup>

Anode	IC area in catholyte @100mA/cm <sup>2</sup> , uS*min	
	Li <sup>+</sup>	Na <sup>+</sup>
Ir	0	1.05
Ir+ Lisicon	0.02	1.15

## Summary

Electrolysis of seawater has been performed to produce hydrogen effectively by employing Ir as the anode, and Pt, Ir and Ni as the cathodes in solid polymer membrane electrolyzer.

1. At low current density, i.e., 10 mA/cm<sup>2</sup>, Pt, Ir and Ni cathodes showed similar activity for hydrogen production. However, at high current density of 100mA/cm<sup>2</sup>, the activity of cathode decreases in the order Ir > Pt > Ni.
2. The current efficiency for hydrogen generation increases with current density; it reaches more than 90% efficiency at 100mA/cm<sup>2</sup> for all the cathodes.
3. Ions diffuse through the membrane during seawater electrolysis. As the concentration of Na<sup>+</sup> ion in seawater is much higher than that of lithium, that Li<sup>+</sup> ion was not separated from Na<sup>+</sup> by ion chromatography.

4. The diffusion of ions depends on the current density; it increases with the current density (or potential). However, the amount of ions diffused was less than 0.1% for all the cathode (Pt, Ir, and Ni) at 100mA/cm<sup>2</sup>.
5. The incorporation of Lisicon in the anode increases the Li<sup>+</sup> ion diffusion. However, the diffusion of Na<sup>+</sup> ions makes it difficult to separate Li<sup>+</sup> ions completely.

### Plans for Next Quarter

The incorporation of Lisicon or Li-adsorbing materials will be made to improve the rate of diffusion of lithium ions. Also, Na<sup>+</sup> ion-conducting membrane will be explored to separate Na<sup>+</sup> ions, prior to the Li<sup>+</sup> extraction step (Figure 10).

The planned activities for next quarter include:

- Prepare Li-adsorbing and conducting materials and incorporate them into the electrolysis cell
- Prepare thin and dense Na<sup>+</sup> selective membranes
- Prepare electrocatalysts on Nafion or ceramic electrolyte to improve the extraction efficiency
- Measure hydrogen gas production along with lithium extraction during the electrolysis
- Optimize the electrochemical Li extraction process

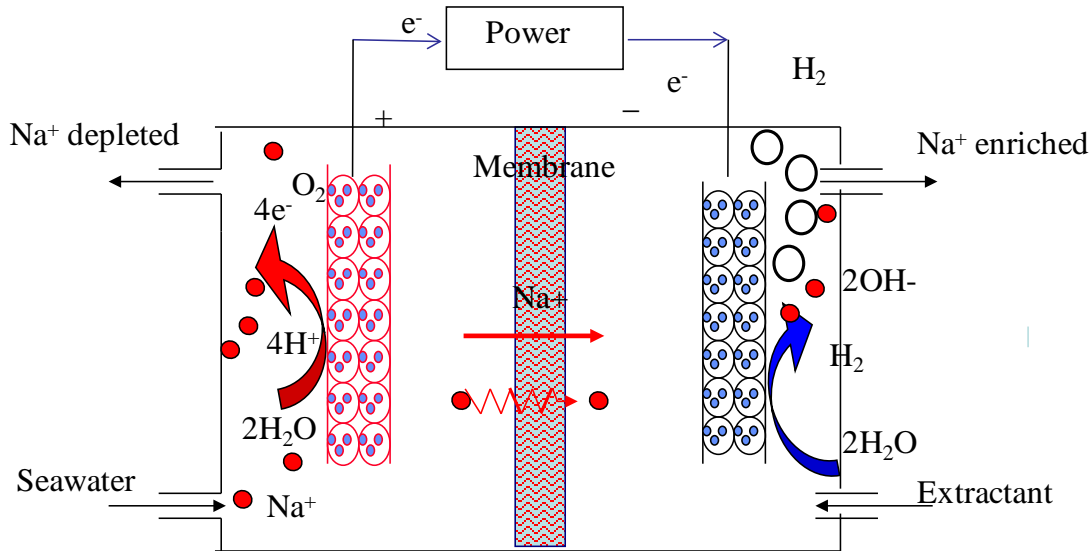


Figure 10. Schematic representation of electrochemical Na<sup>+</sup> separation process.

## References

- [1] J. O.'M. Bockris, Energy, The Solar-Hydrogen Alternative, John-Wiley, NY, 1975.
- [2]. H. K. Abdel-Aal, S. M. Sultan, and I. A. Hussein, Parametric study for saline water electrolysis: Part II- chlorine evolution, selectivity and determination, *Int. J. Hydrogen Energy*, 18, 545-551 (1993).
- [3] H.Y. Song, N. B. Kondrikov, V.G. Kuryavy, Y.H. Kim, Y.S. Kang, Preparation and characterization of manganese dioxide electrodes for highly selective oxygen evolution during diluted chloride solution electrolysis, *J. Ind. Eng. Chem.* 13 (2007) 545.
- [4]. R. Balaji, B. S. Kannan, J. Lakshmi, N. Senthil, S. Vasudevan, G. Sozhan, A. K. Shukla, S. Ravichandran, An alternative approach to selective sea water oxidation for hydrogen production, *Electrochim. Commun.*, 11, 1700-1702 (2009).
- [5] J. E. Bennett, Electrodes for generation of hydrogen and oxygen from seawater, *Int. J. Hydrogen Energy*, 5 (1980) 401.
- [6]. Z. Kato, K. Izumiya, N. Kumagai, and K. Hashimoto, Energy-saving Seawater Electrolysis for Hydrogen Production, *Journal of Solid State Electrochemistry*, 13, 219-224 (2009).
- [7]. K. Fujimura, T. Matsui, H. Habazaki, A. Kawashima, N. Kumagai, and K. Hashimoto, The durability of manganese-molybdenum oxide for oxygen evolution in sea water electrolysis, *Electrochim. Acta*, 45, 2297-2303 (2000).
- [8]. N. A. Abdel Ghany, N. Kumagai, S. Meguro, K. Asami, and K. Hashimoto, Oxygen evolution anodes composed of anodically deposited Mo-Fe oxides for sea water electrolysis, *Electrochim. Acta*, 48, 21-28 (2002).
- [9]. H. Habazaki, T. Matsui, A. Kawashima, K. Asami, N. Kumagai, and K. Hashimoto, Nanocrystalline manganese-molybdenum-tungsten oxide anodes for oxygen evolution in sea water electrolysis. *Scripta Mater*, 44, 1659 (2001).
- [10]. K. Fujimura, T. Matsui, K. Izumiya, A. Kawashima, E. Akiyama, H. Habzaki, A. Kawashima, K. Asami, K. Hashimoto, Oxygen evolution on manganese-molybdenum oxide anodes in sea water electrolysis, *Materials Science and Engineering*, A267, 254-259 (1999).
- [11]. K. Izumiya, E. Akiyama, H. Habzaki, A. Kawashima, K. Asami, K. Hashimoto, and N. Kumagai, Surface activation of manganese oxide electrode for oxygen evolution from seawater, *J. Appl. Electrochemistry*, 27, 1362-1368 (1997).
- [12]. T. Matsui, H. Habazaki, A. Kawashima, K. Asami, N. Kumagai, and K. Hashimoto, Anodically deposited manganese-molybdenum-tungsten oxide anodes for oxygen evolution in seawater electrolysis, *J. Appl. Electrochemistry*, 32, 993-1000 (1997).
- [13]. K. Fujimura, K. Izumiya, A. Kawashima, E. Akiyama, H. Habzaki, N. Kumagai,, and K. Hashimoto, Anodically deposited manganese-molybdenum-tungsten oxide anodes with high activity for evolving oxygen in electrolysis of seawater, *J. Appl. Electrochemistry*, 29, 765-771 (1999).
- [14]. P. B. Stewart and P. Munjal, Solubility of carbon dioxide in pure water, synthetic seawater, and synthetic seawater concentrates at -5°C to 25°C and 10 to 45 atm. pressure, *J. Chemical & Engineering Data*, 15, 67-71 (1970).
- [15]. F. Rosalbino, S. Delsante, G. Borzone, and E. Angelini, Correlation of microstructure and catalytic activity of crystalline Ni–Co–Y alloy electrode for the hydrogen evolution reaction in alkaline solution, *J. Alloys and Compounds*, 429, 270-275 (2007).

- [16]. R. Solmaz, A. Döner, and G. Kardaş, The stability of hydrogen evolution activity and corrosion behavior of NiCu coatings with long-term electrolysis in alkaline solution, *Int. J. Hydrogen Energy*, 34, 2089-2094 (2009).
- [17]. F. Rosalbino, G. Borzone, E. Angelini, and R. Raggio, Hydrogen evolution reaction on Ni-RE (RE= rare earth) crystalline alloys, *Electrochim. Acta*, 48, 3939-3944 (2003).
- [18]. S. P. Singh, R. N. Singh, G. Poillearat, and P. Chartier, Physicochemical and electrochemical characterization of active films of LaNiO<sub>3</sub> for use as anode in alkaline water electrolysis, *Int. J. Hydrogen Energy*, 20, 203-210 (1995).
- [19]. N. Jiang, H-M. Meng, L-J. Song, and H-Y. Yu, Study on Ni-Fe-C cathode for hydrogen evolution from seawater electrolysis, *Int. J. Hydrogen Energy*, 35, 8056-8062 (2010).
- [20]. A.A. El-Moneim, J. Bhattacharai, Z. Kato, K. Izumiya, N. Kumagai, and K. Hashimoto, Mn-Mo-Sn oxide Anodes for oxygen evolution in sea-water electrolysis for hydrogen production, *ECS Trans.*, 25, 127-137 (2010).